Water Science & Technology

IWA PUBLISHING

Water Science & Technology Vol 85 No 6, 1840 doi: 10.2166/wst.2022.078

Heterogeneous degradation of amoxicillin in the presence of synthesized alginate-Fe beads catalyst by the electro-Fenton process using a graphite cathode recovered from used batteries

Hakima Kadji [a,*], Idris Yahiaoui [a], Fadila Akkouche [a], Farouk Boudrahem [a], Sonia Ramdani[a], Anissa Saidane[a], Amar Manseri[b], Abdeltif Amrane [c] and Farida Aissani-Benissad [a]

[a] Laboratoire de Génie de l'Environnement (LGE), Faculté de Technologie, Université de Bejaia, Bejaia 06000, Algeria
[b] Centre de Recherche en Technologie des Semi-conducteurs pour l'Energétique, CRTSE: 02 Bd Frantz Fanon, Alger B.P 140, Algeria
[c] Univ Rennes, Ecole Nationale supérieure de Chimie de Rennes, CNRS, ISCR – UMR 6226, Rennes F-35000, France
*Corresponding author. E-mail: hakima.kadji@univ-bejaia.dz

HK, 0000-0003-4684-4447; IY, 0000-0002-4400-2900; FA, 0000-0002-0673-5476; FB, 0000-0002-4378-8147; AA, 0000-0003-2622-2384; FA-B, 0000-0002-6214-9922

ABSTRACT

Iron alginate beads (Fe-Alg) were prepared, characterized and implemented for the degradation of amoxicillin (AMX) by the heterogeneous electro-Fenton process using a graphite cathode recovered from used batteries. Scanning electron microscopy (SEM) showed that (Fe-Alg) beads have a spherical shape and the results of energy dispersive spectrometric (EDS) revealed the presence of iron in (Fe-Alg). Optimization of the operating parameters showed that a complete degradation of AMX was achieved within 90 min of heterogeneous electro-Fenton treatment by operating under these conditions: initial AMX concentration: 0.0136 mM, I = 600 mA, $[Na_2SO_4] = 50$ mM, pH = 3, T = 25 °C, $\omega =$ 360 rpm. The corresponding chemical oxygen demand (COD) abatement was 50%. Increasing the contact time increased the COD abatement to 85.71%, after 150 min of heterogeneous electro-Fenton treatment. The results of the kinetic study by using nonlinear methods demonstrated that the reaction of AMX degradation obeyed to a pseudo-second-order kinetic. Iron content of 4.63% w/w was determined by the acid digestion method. After 5 cycles of use, the Alg-Fe catalyst depletion was only 8%. Biodegradability was remarkably improved after electro-Fenton pretreatment, since it increased from 0.07 initially to 0.36. The heterogeneous electro-Fenton process had efficiently eliminated AMX and it increased the biodegradability of the treated solution.

Key words: alginate beads, amoxicillin, electro-Fenton, graphite, hydroxyl radicals

HIGHLIGHTS

- The heterogeneous electro-Fenton process was used for the degradation of amoxicillin (AMX).
- The Fe-Alg catalyst has proved its efficiency and stability.
- The kinetic model of the AMX degradation obeyed to a pseudo-second-order.
- The COD abatement and removal yield of AMX were 50% and 100% respectively.
- The heterogeneous electro-Fenton pretreatment improved the biodegradability of the AMX from 0.07 initially to 0.36.

GRAPHICAL ABSTRACT

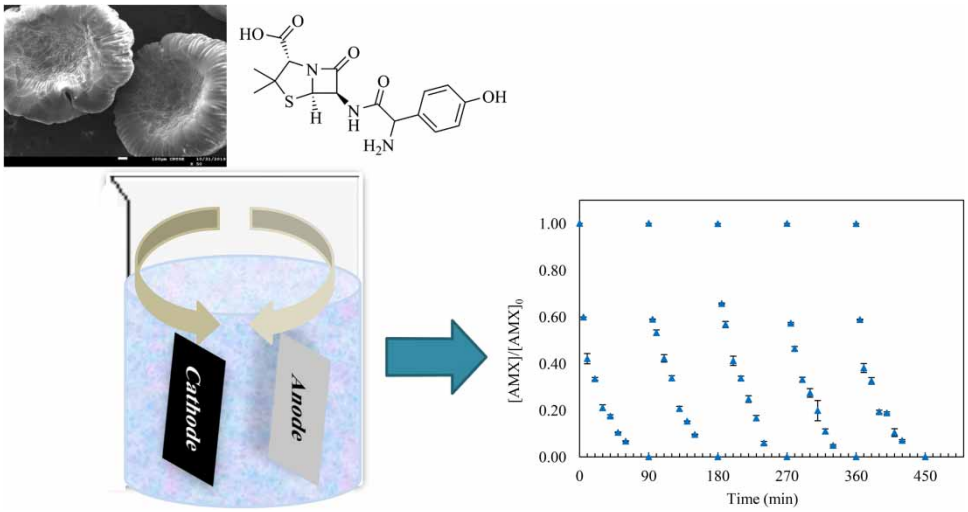

INTRODUCTION

The presence of human antibiotics in the environment has become a serious environmental concern. The concentrations of these compounds have been reported to be in the range of $\mu g/L$ (Elizalde-Velázquez *et al.* 2016). Even at low concentrations, the presence of antibiotics in surface and groundwater constitutes a great threat for the ecosystem (Kadji *et al.* 2021). Thus, exposure to antibiotics can lead not only to growth stunting and bodyweight reduction in aquatic organisms, but also to the development of antibiotic resistance genes in pathogenic bacteria, which constitutes a dangerous threat to human health, since the effectiveness of the treatment of bacterial infections is reduced (Kumar *et al.* 2021). The beta lactams represent the major pharmaceutical products; they constitute 65% of the world market for antibiotics (Mojiri *et al.* 2019). Among them, amoxicillin (AMX) is a broad-spectrum beta-lactam antibiotic, and it is one of the most prescribed antibiotics. AMX is widely used for the treatment of a variety of bacterial infections. However, about 60% of the prescribed and taken AMX is excreted unchanged (Dogan & Kidak 2016) and hence is released in wastewater. This presents a potential risk for the environment and human beings (Li *et al.* 2015). Chemical and physicochemical techniques have been widely studied to remove antibiotics from water such as adsorption (Boudrahem *et al.* 2019; Saidi *et al.* 2019; Akkouche *et al.* 2021). Adsorption is one of the most effective and low-cost methods, but this technique has some disadvantages such as being non-destructive and merely transferring pollutants from one phase to another, which always results secondary pollution (Madi-Azegagh *et al.* 2018a, 2018b). The biological methods such as activated sludge process and anaerobic treatment, the most cost-effective for wastewater treatment, which are destructive and have been extensively studied, do not always appear relevant for the removal of pollutants, owing to their low biodegradability (Ikhlef-Taguelmimt *et al.* 2020; Kadji *et al.* 2021). However, these techniques are not adapted for the treatment of antibiotics residues owing to their recalcitrance (Annabi *et al.* 2016; Dogan & Kidak 2016).

Among the most recent progress in the treatment of water, advanced oxidation processes (AOPs) have gained growing attention (Taoufik *et al.* 2021), including photocatalysis (Aissani *et al.* 2018), electrochemistry (Yahiaoui *et al.* 2016; 2018) and electro-Fenton (Kadji *et al.* 2021). These techniques are very interesting for the destruction of toxic and non-biodegradable molecules because they allow a thorough elimination of the pollutant with a decrease of the overall toxicity of the treated effluent (Ammar *et al.* 2015). These processes are based on the formation of a potent reactive oxygen species, the hydroxyl radical $HO^{\cdot}$, which is the most powerful oxidizing specie after fluorine (Li *et al.* 2015). Among them, the Fenton process is an AOP applied for the decontamination of wastewater containing significant concentrations of recalcitrant organic micropollutants (Annabi *et al.* 2016). Nevertheless, it has some disadvantages, namely (i) The production of waste iron sludge, which has to be subsequently eliminated (ii) the use of a large amount of hydrogen peroxide (iii) The consumption of hydrogen

peroxide by radical scavenging reaction (Equation (1)) (Mirzaei *et al.* 2017).

$$H_2O_2 + HO^{\cdot} \rightarrow H_2O + HO_2^{\cdot} \quad (1)$$

To overcome these disadvantages, it is worth considering Fenton-based processes such as the electro-Fenton process. In this case, the well-known Fenton's reactant H_2O_2/Fe^{2+} is *in situ* generated from electrode reactions, avoiding the need for the external addition of Fenton's reactant. The cathodic reduction of ferric ions ensures the regeneration of ferrous ions (Equation (2)); this avoids the addition of large amounts of iron to the reaction medium. Hydrogen peroxide electrosynthesis occurs at the cathode in the presence of both oxygen contained in air feeding and oxygen generated on the anode surface by the decomposition of water (Equation (3)). Hydroxyl radicals are produced *in situ* in the reaction medium according to the Fenton's reaction (Equation (4)) (Annabi *et al.* 2016).

$$Fe^{3+} + e^{-} \rightarrow Fe^{2+} \quad (2)$$

$$O_2 + 2H^{+} + 2e^{-} \rightarrow H_2O_2 \quad (3)$$

$$H_2O_2 + Fe^{2+} \rightarrow Fe^{3+} + HO^{\cdot} + HO^{-} \quad (4)$$

Recently, scientists give more importance to heterogeneous electro-Fenton process, which is considered as an environmentally friendly approach, since the catalyst is supported on a solid material. This permits easy separation and recovery of the catalyst and minimizes the production of waste sludge (Zárate-Guzmán *et al.* 2019).

This study, in great detail, focused in a first part on the recovery of graphite rod from used batteries to use it as a cathode in the electro-Fenton process, since the graphite cathode is the best material for H_2O_2 electro-generation (Nayebi & Ayati 2021) and to reduce the electrode cost. In a second part, the immobilization of iron in the biomaterial by using alginate beads, which rectifies some of the disadvantages of the conventional electro-Fenton process. Furthermore, the efficiency of iron alginate beads (Fe-Alg) and the graphite rod for the degradation of AMX by the heterogeneous electro-Fenton treatment was tested. For this purpose, the effects of operational parameters such as the applied current intensity, the temperature and the initial AMX concentration on the degradation of AMX were studied.

EXPERIMENTAL AND METHODS

Disassembling the used battery

One of the most toxic and chemical-rich wastes is used batteries. The implementation of measures for the control of these waste batteries is still insufficient in developing countries; furthermore, techniques for the recycling of this waste are not yet available. The electrode is made of graphite, and has many applications if we mention only a few: it is used as a lubricant in motor oils, it is used as a mould in the manufacture of mineral compounds (ferro-alloys), and it is also used in pencil mines. The aim of this study is therefore to recover the electrode to use it as a cathode in the electro-Fenton process. The samples to be studied are cylindrical R20 batteries with an electromotive force of 1.5 V (32 mm × 61 mm). The steps for dismantling the used battery are listed below:

- Use the screwdriver to remove the plastic cover.
- Saw off the top part along its width in order to remove the plastic cover and the cap.
- Saw the casing lengthwise to remove the top part, remove the washer and then the plastic layer to access the black powdery mixture between the zinc cylinder and the graphite electrode.
- Recover the graphite electrode (see figure S1, supplementary material), wash it and sand it with abrasive paper.'

Chemicals

The target compound was amoxicillin ($C_{16}H_{19}N_3O_5S$) with purity of 99%; it was purchased from Sigma-Aldrich and its characteristics are presented in table S1 (supplementary material). Na_2SO_4 (99% purity), H_2SO_4 (96% purity), $Fe_2O_{12}S_3$ (96% purity), $CaCl_2$ (96% purity), CH_4O (99% purity), KH_2PO_4 (99.5% purity), and sodium acetate anhydrous (99% purity) were purchased from Biochem Chemopharma. Sodium alginate and 1,10- phenanthroline (99% purity) were obtained from Sigma-Aldrich. hydroxylamine hydrochloride ($NH_2OH{\cdot}HCl$, 98% purity), was purchased from Labosi.

Two electrodes (see description in our previous work (Kadji *et al.* 2021) were connected to a DC supply (Model GW insTEK GPS-2303) and an electric field was applied. All electrolyses were carried out in a 600 mL undivided cylindrical Pyrex glass cell (see figure S2, supplementary material). The electrodes were centred in the bulk, the inter-electrode distance was 1 cm. The synthetic aqueous solutions treated were prepared by dissolving a certain amount of AMX in distilled water (2.5, 5 and 15 mg of AMX was used to prepare a solution with a concentration of 0.0136, 0.027 and 0.082 mM, respectively). And then the pH solution was adjusted to 3 using sulphuric acid. Prior to the electro-Fenton experiment, the solution was saturated by oxygen contained in the air by means of a pump, and then 3.1 g of Alg-Fe beads were added to the electrolysis cell.

Alg-Fe beads synthesis

Numerous research papers report the synthesis of Alg-Fe beads as catalyst, employing different conditions and preparation methods (Rosales *et al.* 2012; Iglesias *et al.* 2014; Hammouda *et al.* 2016).

The Alg-Fe beads were prepared by extrusion (see figure S3, supplementary material). A mixture containing the gelation agent, calcium chloride (2% w/v) and the solution of sulfate iron was prepared and maintained under vigorous stirring. The concentration of ferric ions in the solution was 0.02 M. The synthesis of the alginate beads was ensured by dropwise addition of alginate sodium solution (3% w/v) to the solution containing the crosslinking agent using a syringe. A rapid reaction occurred between the alginate and the crosslinking agent on the surface, leading to instantaneous formation of beads with spherical shape. The drip was done through a needle of 3 mm internal diameter.

The maturation time of alginate beads was fixed to 24 hours. This period is largely sufficient to ensure complete gelation of the alginate. After that, the beads were filtered and washed with distilled water to remove excess chloride and calcium ions. Wet beads obtained were dried at 40 °C during 48 h.

Scanning electron microscopy (SEM)

Surface morphology of beads was analysed with scanning electron microscopy (SEM) coupled to energy dispersive spectrometric (EDS) to determine the chemical composition of the beads (model JOEL JSM7_7610F PLUS).

Iron content and concentration

Based on related studies (Hammouda *et al.* 2016), the total iron contained in the beads was determined by acid digestion using concentrated sulfuric acid. The colorimetric o-phenanthroline method was used to determine the concentration of iron; 1,10-phenanthroline reacts with the ferrous ion Fe^{2+} to form the tris (1,10-phenanthroline) Fe II, also called ferroin: $[Fe(o\text{-}phen)3]^{2+}$, a red-orange complex. The absorbance was measured at $\lambda = 510$ nm by UV visible spectrophotometer (Thermo-scientific evolution 2001). The full method was described by Saywell & Cunningham (1937). This method was used to determine the iron concentration during the treatment and the iron content in the beads.

ANALYTICAL METHODS

AMX analysis

The quantification of the concentration of AMX was determined by high performance liquid chromatography (HPLC ACC 3000 HPLC). Samples were taken and filtered through 0.22 μm membrane syringe filter (Satorius Stedim biotech Gmbh, Germany). The HPLC was equipped with a standard degasser (LPG 3400 SD), an autosampler, pump (Model LPG 3400 SD) and a detector with visible ultraviolet ray (UV/Vis detector VWD 3400 RS). The separation was achieved on a Thermo Fisher scientific (Germany) C18 (5 mm; 4.6 × 150 mm) reversed-phase column. The mobile phase consisted of CH_4O/KH_2PO_4 (5/95 v/v) with a flow rate of 0.5 mL/min and the detection of AMX was carried out at 232 nm.

Chemical oxygen demand and BOD_5 measurements

All BOD_5 measurements were duplicated and average results were used. The determination of BOD_5 was carried out in Oxitop in the presence of added nutrients according to EN 1899-1-H51. Additionally, the probable influence of nitrification processes was inhibited by N-allythiourea. The incubation of the samples was carried out directly in Oxitop in the presence of activated sludge from a waste treatment plant (Sidi Ali Labhar, Béjaia, Algeria) and the determination of oxygen dissolved in water was carried out after 5 days at 20 °C. The chemical oxygen demand (COD) was measured by means of Kits Nanocolor® 15–160 mg/L COD according to DIN ISO 15705 at 148 °C. The amount of oxygen required for the oxidation of the organic

and mineral matter at 148 C for 2 h was quantified after oxidation with $K_2Cr_2O_7$ at acidic pH and heating. COD was measured by Nanocolor 500D photometer type (Macherey-Nagel, Hoerd, France) (Yahiaoui *et al.* 2016, 2018).

THEORY CALCULATION

Activation energy

The energy activation value required for the reaction of AMX's degradation under the heterogeneous electro-Fenton process was appraised. The slope of the line giving the variation of $\ln(k_{app})$ versus (1/T) was assessed using Arrhenius' law (Equation (5)).

$$k_{app} = A\ exp^{\frac{-Ea}{RT}} \tag{5}$$

where: A is a pre-exponential factor; E_a is the apparent energy activation (J/mol); T is the reaction temperature (K); R = 8.314 (J/mol. K).

Kinetic study

To determine the kinetic model, which appropriately describes the degradation reaction of AMX, first- (Equation (6)) and second-order models (Equation (7)) were tested.

$$r = -\frac{dC}{dt} = k_1 C \tag{6}$$

$$r = -\frac{dC}{dt} = k_2 C^2 \tag{7}$$

where: C is the concentration of AMX at a given time (mg/L), r is the rate of AMX degradation (mg/L.min), k_1 (min^{-1}) and k_2 (L/mg.min) are the first-order and second order rate constants, respectively.

The non-linear method was considered to establish the kinetic models (Kadji *et al.* 2021). The solver in Microsoft Excel permitted the determination of the minimum of the D function (Equation (8)); therefore, the rate constants were calculated.

$$D(\%) = \sum_{i=1}^{p} \left(\frac{C}{C_0}|_{Exp} - \frac{C}{C_0}|_{Cal} \right)^2 \tag{8}$$

where: p is the number of experimental data, C_{0Cal} and C_{0Exp} are the calculated and experimental data respectively (mg/L).

RESULTS AND DISCUSSION

Iron content

Calculation of the iron retained in the alginate revealed that the composition in iron beads was 4.63% w/w.

Characterization of beads

The images in Figure 1(a) and 1(c) show that all beads have a spherical shape, in agreement with the related literature (Fundueanu *et al.* 1999; Rosales *et al.* 2012). The iron-free alginate (Alg) beads (Figure 1(a) and 1(b)) have a homogeneous and smooth surface with undulations. On the opposite, a change in the texture of the alginate-iron beads (Alg-Fe) was noticed as it is illustrated in Figure 1(c)–1(e), due most likely to the presence of iron in the Alg-Fe beads. These beads had a rough- and heterogeneous surface with less apparent fissures or fractures. This difference in texture shows that the iron interacted and was efficiently dispersed in the alginate beads by modifying their initial texture through physico-chemical interactions.

The composition of iron, calcium and sodium contained in the beads was determined by EDS. The results of this analysis for the different synthesized beads (Alg and Alg-Fe) are depicted in Figure 2. The EDS spectrum of iron-free alginate beads Figure S4(a) showed a significant peak of calcium, while the peak sodium ions was very weak. Indeed, the sodium ions initially present in the alginate were replaced by Ca^{2+} ions by ion exchange. The analyses performed on the Alg-Fe beads

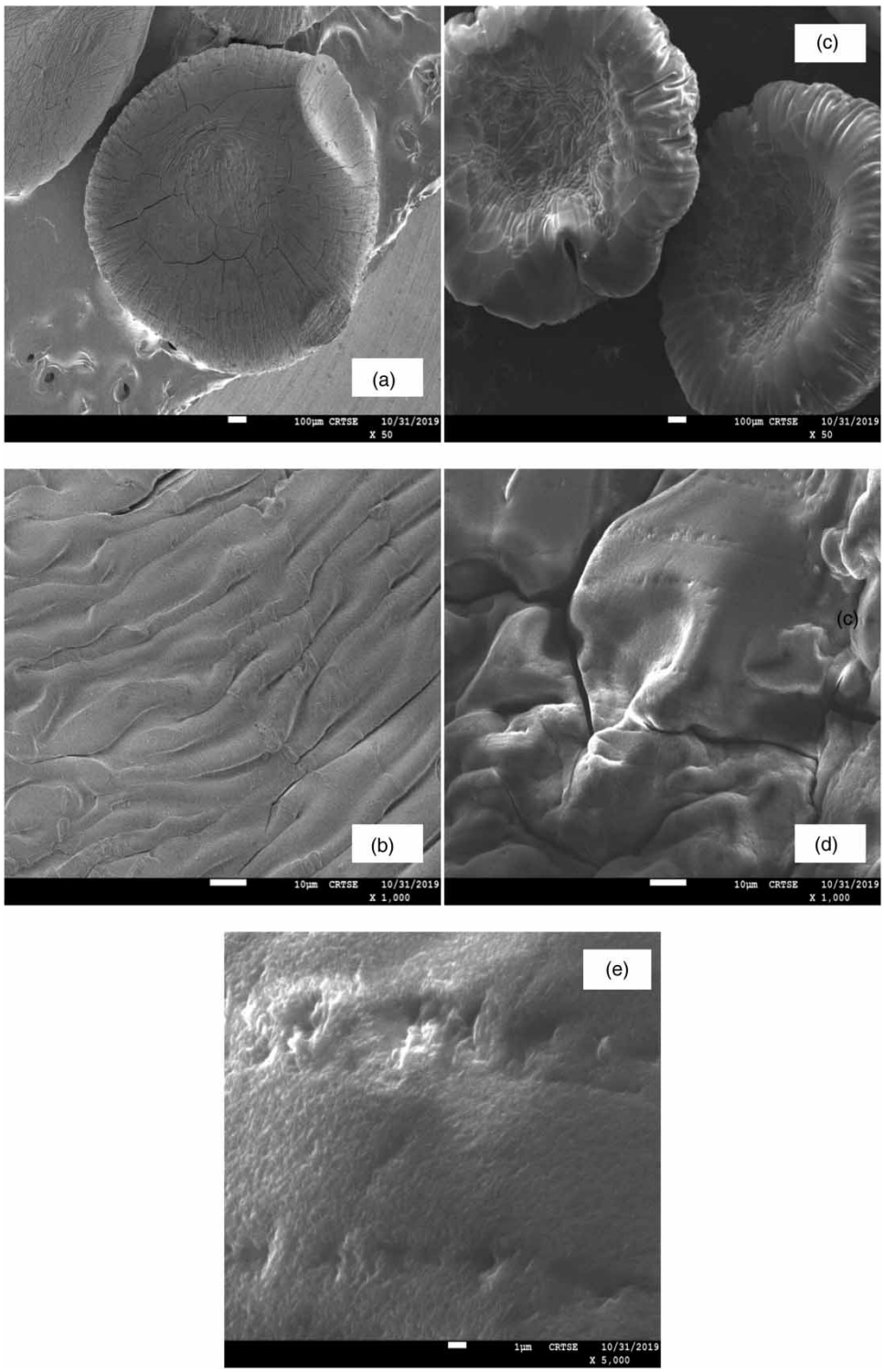

Figure 1 | SEM images of alginate beads without encapsulated iron (Alg beads); (a), (b), and alginate beads with encapsulated iron (Alg-Fe beads); (c), (d), (e).

are shown in Figure 2(b). The spectrum shows the presence of iron in the sample and the absence of calcium, while some of the sodium ions were still present Figure S4(b), but the remaining amount was almost insignificant. This difference in composition shows that the iron encapsulation was effective.

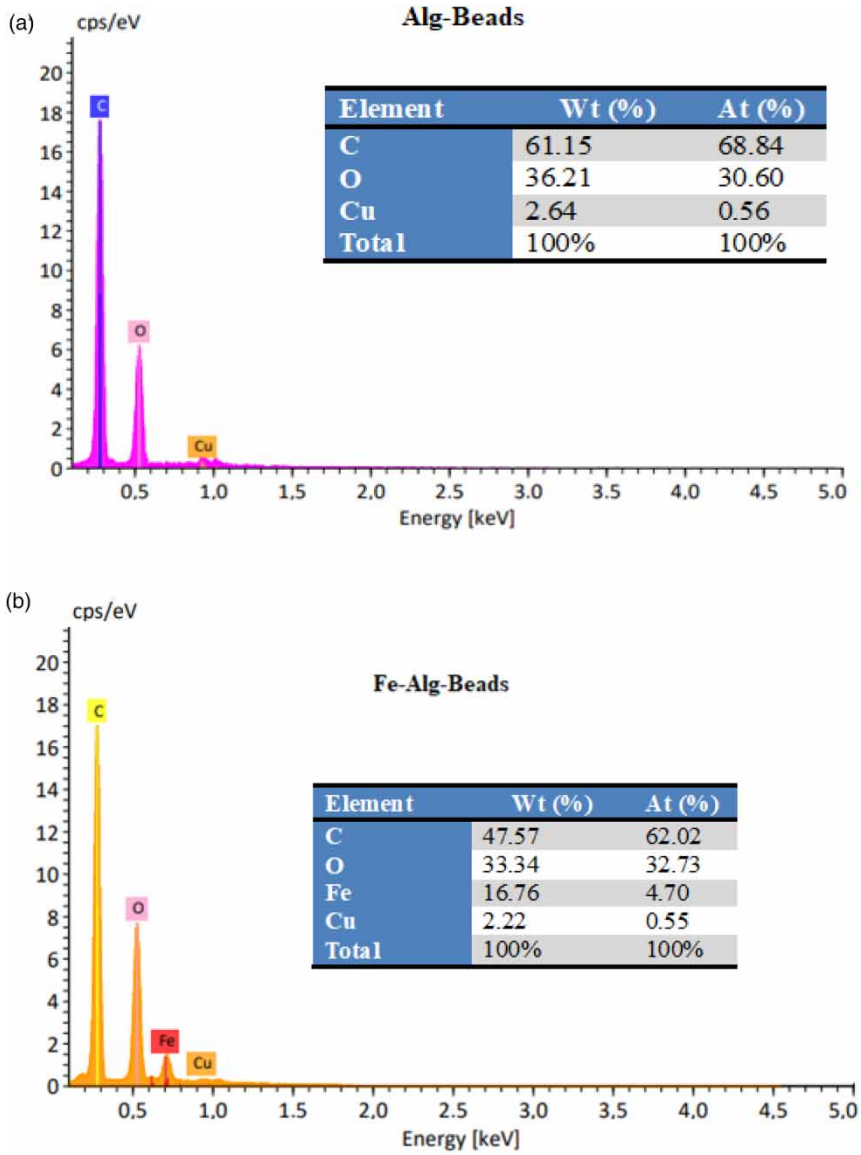

Element	Wt (%)	At (%)
C	61.15	68.84
O	36.21	30.60
Cu	2.64	0.56
Total	100%	100%

Element	Wt (%)	At (%)
C	47.57	62.02
O	33.34	32.73
Fe	16.76	4.70
Cu	2.22	0.55
Total	100%	100%

Figure 2 | EDS spectrum of alginate beads: (a) alginate beads without encapsulated iron (Alg beads); (b) alginate beads with encapsulated iron (Alg-Fe beads).

Adsorption of AMX on the catalyst

The adsorption test was performed in the dark. A synthetic solution of 0.082 mM AMX was prepared. The pH was adjusted to 3 since the optimum pH value for the Fenton reaction is about 3. According to previous research studies on the electro-Fenton process, it is found that acidic pH values close to 3 are the most favourable for the electro-Fenton oxidation (Huang *et al.* 2017; Rezgui *et al.* 2018), in fact, iron acts as a catalyst with maximum catalytic activity at acidic pH (Miklos *et al.* 2018). Thus, the oxidation potential of hydroxyl radicals decreases with increasing pH. This is due, on the one hand, to the fact that the decomposition of H_2O_2 into water and oxygen is accelerated at pH values above 5 and, on the other hand, to the formation of ferric hydroxides at a pH above 4, which reduces the degradation rate (Ghanbari & Moradi 2015; Aramyan & Moussavi 2017; Mirzaei *et al.* 2017). The catalyst was added to the reaction medium after pH adjustment. After 150 min the removal yield was only 1%; this clearly indicates that adsorption can be neglected, the same findings were reported by Rosales *et al.* (2012) and Hammouda *et al.* (2016) using Alg-Fe beads as catalyst in the the electro-Fenton process for the decolourisation of dyes and the degradation of indole, respectively.

Effect of the applied current intensity

The first parameter examined was the influence of the current intensity, since it exerts a significant effect on the degradation ability of the EF-Alg-Fe process (Electro-Fenton Alg-Fe process) (Mansour *et al.* 2012; Annabi *et al.* 2016). Trials were performed by varying the applied current intensity from 50 to 600 mA. The Figure 3(a) exemplified the results of AMX removal. The degradation yield was improved as the current intensity increased, from 86.22% to an almost total degradation at 400 mA, which should be related to a higher production of •OH in the system. In addition, increasing the current intensity should lead to an improvement of the ferrous ion regeneration by cathodic reduction. Accordingly, the COD abatement also increased (Figure 3(b)) with the current intensity, until 82.35% for 600 mA. Meanwhile, the optimal operating current intensity was 600 mA.

The variation in iron concentration as a function of the applied electric current was followed during treatment (see figure S5, supplementary material). The results indicated that the increase in current intensity in the 50–600 mA range strongly affects the total iron concentration. Indeed, the amount of iron increased with current intensity, from a negligible amount for 50 mA to79.71 mg·L^{-1} for 600 mA. This significant increase of iron concentration observed is probably due to the fact that the release of iron from the beads is favored at high current intensities. The amount of ferrous ions released into the solution increased at high currents leading to an increase in the number of •OH radicals, which is associated with an increase in the COD abatement rate. This suggests that a homogeneous fenton reaction has been occurred (Mirzaei *et al.* 2017).

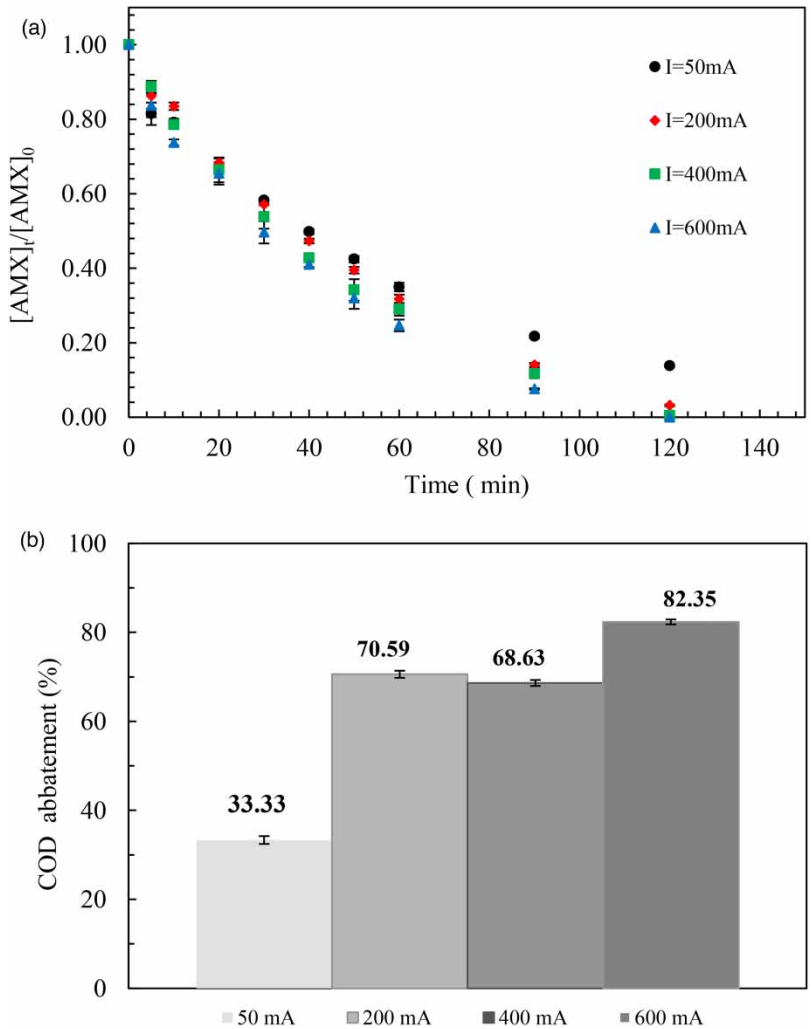

Figure 3 | Influence of the current intensity on the degradation of AMX. Conditions: $[AMX]_0 = 0.082$ mM, $[Na_2SO_4] = 50$ mM, pH = 3, T = 25 °C, $\omega = 360$ rpm. (a) AMX's degradation, (b) COD abatement.

Effect of the temperature

To check the influence of this parameter on the AMX's degradation, assays were carried out at 25, 45 and 55 °C, leading to an almost total removal after 120 min of reaction time in the range of temperatures tested, as evidenced by Figure 4(a). However, a slight increase of the degradation rate for increasing temperatures should be noted, as it is confirmed at the examination of the rate constant, the values were 0.023, 0.0269, and 0.0292 for 25, 45, and 55 °C, respectively.

It can be seen from Figure 4(a), the increase of the temperature did not significantly improve the AMX's removal and irrespective of the temperature total removal was observed at 120 min reaction time. This might be attributed to the decomposition of hydrogen peroxide to oxygen and water at high temperatures according to (Equation (9)) (Mirzaei *et al.* 2017). In addition, oxygen dissolution diminishes as the temperature rises, so less hydrogen peroxide is produced via (Equation (3)) (Mansour *et al.* 2012); this slows down the Fenton's reaction, and subsequently there are fewer hydroxyl radicals in the solution. Moreover, high temperatures may deteriorate the catalyst to small fragments (Mirzaei *et al.* 2017).

As a result, a temperature of 25 °C was considered thereafter.

$$2H_2O_2 \rightarrow 2H_2O + O_2 \quad (9)$$

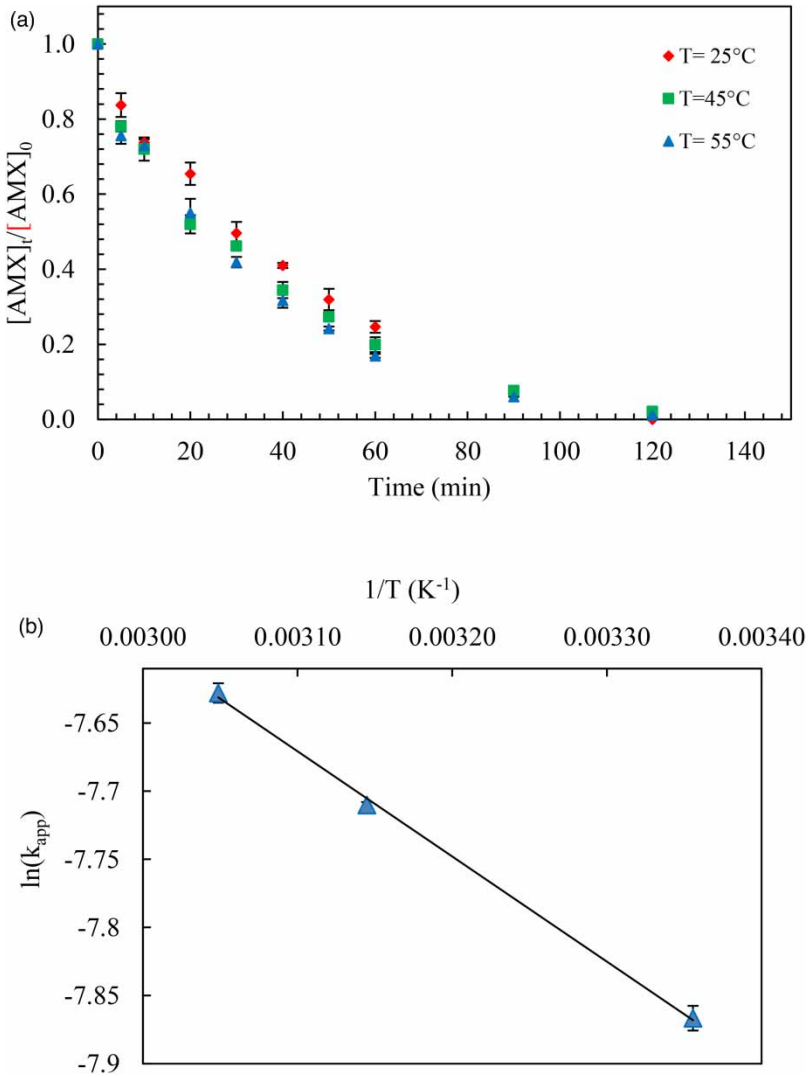

Figure 4 | (a) Influence of the temperature on the degradation of AMX. Conditions: I = 600 mA, $[AMX]_0 = 0.082$ mM, $[Na_2SO_4] = 50$ mM, pH = 3, $\omega = 360$ rpm. (b) The variation of ln k_{app} versus 1/T for the degradation of AMX by the EF process. Conditions: I = 600 mA, $[AMX]_0 = 0.082$ mM, $[Na_2SO_4] = 50$ mM, pH = 3 $\omega = 360$ rpm.

The variation of iron concentration at different temperatures was examined. The total iron concentration after 120 min of reaction time was 79.71 and 76.19 mg·L^{-1} for 25 and 45 °C, respectively, which does not show a significant impact between 25 and 45 °C; while further increase to 55 °C considerably increased the iron concentration to 108.12 mg·L^{-1}. The increase in iron concentration at a high temperature could be attributed to the increased leaching of iron from the beads into the solution, as ferric ions are easily leached from the beads at high temperature. In addition, we found that the apparent degradation rate constants increased with temperature. This can be explained that degradation takes place by the homogeneous Fenton reaction resulting from the presence of high concentrations of iron in the solution (Mirzaei *et al.* 2017).

Energy activation

The line giving the variation of ln(k_{app}) versus (1/T) is illustrated in Figure 4(b). The energy of activation was found to be 6.42 KJ/mol. It is in agreement with the activation energy value (7.5 kJ/mol) reported by Mansour *et al.* 2012, for the degradation of sulfamethazine by electro-Fenton process. Some researchers calculated the activation energy for the degradation of some refractory organic compounds by using a dark Fenton-like process, a photo Fenton-like process (Ifelebuegu *et al.* 2016) and thermally activated persulfate (Zhao *et al.* 2019); the results were 104 kJ/mol, 42 kJ/mol and 126.9 kJ/mol, respectively. Comparison of these values to the one found in this study allowed to conclude that a low energy is enough to realize the degradation's reaction of AMX by a heterogeneous electro-Fenton process.

Effect of the initial AMX concentration

Concerning the effect of the initial AMX concentration, the results obtained by conducting experiments at 0.082 and 0.027 and 0.0136 mM are represented in Figure 5. As observed, the degradation rate of the AMX was inversely proportional to its initial concentration. Indeed, for 0.0136 mM the degradation rate was 100% within 90 min of reaction time. The time became longer with higher AMX concentration, as revealed for 0.027 and 0.082 mM, the AMX disappeared only after 120 min of treatment, which is expected because more organic matter is oxidized by the same amounts of generated hydroxyl radicals, causing then competitive consumption of hydroxyl radicals between intermediate products and the target molecule.

Kinetic study

Based on the kinetic results illustrated in Figure 6 and Table 1, the curves (Figure 6(a) and 6(b)) suggest that the model of pseudo-first order kinetic was the most appropriate for the concentrations of 0.082 and 0.027 mM. These results are in an agreement with other research studies carried out on the degradation of refractory organic compounds by the heterogeneous electro-Fenton process, which employed different catalysts and showed that the degradation kinetic follows a pseudo-first-order model (Kalantary *et al.* 2018; Liu *et al.* 2018). In addition, the calculated first-order rate constants in this study are in the same range compared to other studies. For example, Kalantary *et al.* (2018), in their study of AMX degradation by a heterogeneous electro-Fenton process using Nano-Fe_3O_4 as a catalyst, indicated that 89.1% of AMX was degraded in 1 h of reaction time, with a rate constant of 0.0457 min^{-1}. Liu *et al.* (2018) treated a pharmaceutical contaminant, ibuprofen using iron supported on activated carbon fiber cathode, the rate constant was determined to be 0.0288 min^{-1}. Otherwise,

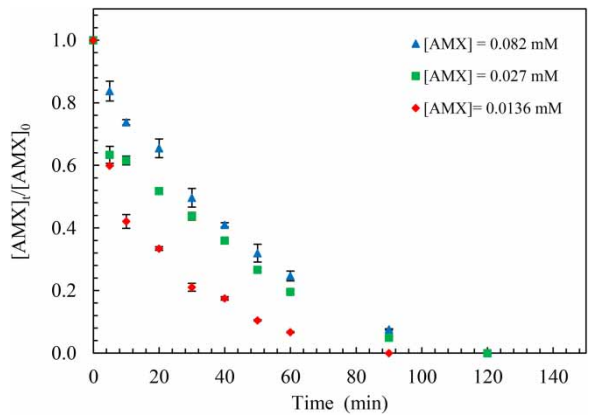

Figure 5 | Influence of the initial concentrations of the AMX on the degradation of AMX. Conditions: I = 600 mA, [Na_2SO_4] = 50 mM, pH = 3, T = 25 °C, ω = 360 rpm.

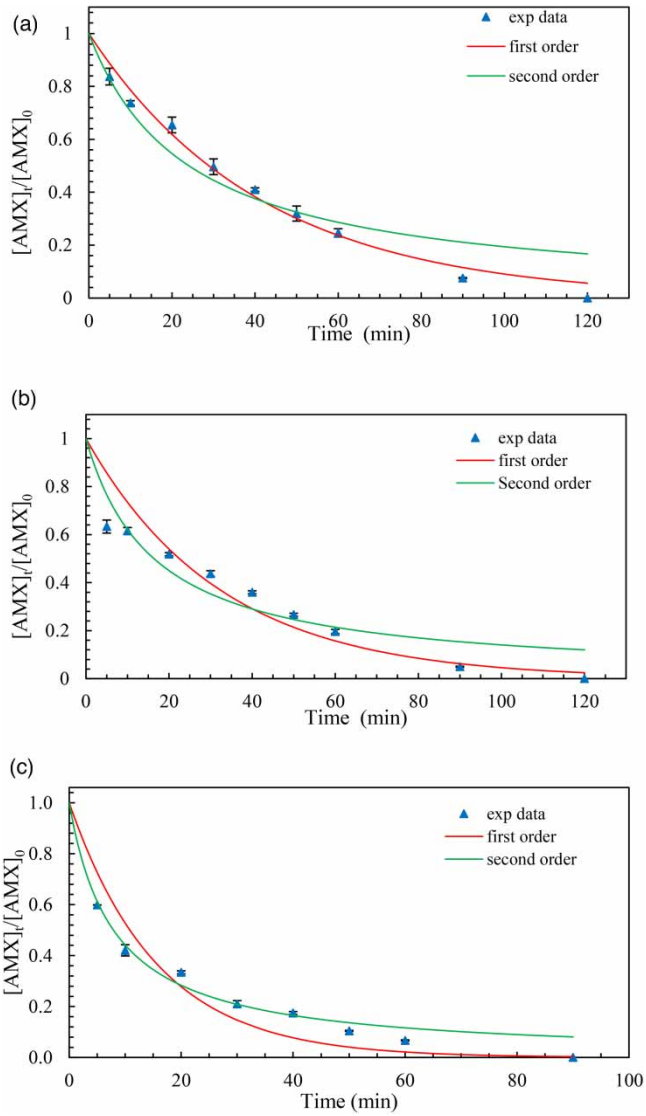

Figure 6 | Experimental data, first-order kinetic model and second-order kinetic model for the degradation of the AMX. Conditions: I = 600 mA, $[Na_2SO_4]$ = 50 mM, pH = 3, T = 25 °C, ω = 360 rpm. (a) $[AMX]_0$ = 0.082 mM, (b) $[AMX]_0$ = 0.027 mM, (c) $[AMX]_0$ = 0.0136 mM.).

Table 1 | Rate constants, D (%) and R^2 values

	First order kinetic model			Second order kinetic model		
Initial AMX concentration (mM)	**k_1 (min^{-1})**	**R^2**	**D (%)**	**k_2 (L/mg.min)**	**R^2**	**D (%)**
0.082	0.0240	0.98	1.2	0.0016	0.86	6.4
0.027	0.0308	0.9	7.6	0.0065	0.86	6
0.0136	0.0640	0.91	4.8	0.0270	0.95	0.4

hydroxyl radicals do not accumulate in the reaction medium (Antonin *et al.* 2015), since they are very reactive species, with very short half-life (10^{-3} µs) (Antonin *et al.* 2015; Mirzaei *et al.* 2017).

As presented in Table 1, it is worth noting that the kinetic degradation of AMX was impacted by the initial concentration of AMX; the rate constant of degradation diminished as the initial concentration of AMX increased. The same observations were reported in the literature studies (Mansour *et al.* 2012; Annabi *et al.* 2016). This behaviour results, on the one hand,

from the non-selectivity of the hydroxyl radicals that react with the target pollutant and the generated intermediate compounds. On the other hand, the amount of produced hydroxyl radicals is constant, while the quantity of organic molecules present in the solution bulk increases (Annabi *et al.* 2016).

Alg-Fe beads stability and renewability

The reusability of the Alg-Fe catalyst was studied. To reveal the impact of this crucial factor, assays were conducted in the optimal operating conditions. As illustrated in Figure 7, the degradation efficiency after each cycle was nearly similar to that of the first cycle; after 5 cycles of use, the Alg-Fe catalyst depletion was only 8%. Based on these results, the performance of Alg-Fe catalyst was demonstrated.

Biodegradability test

To assess the biodegradability after the electro-Fenton process, the BOD_5/COD ratio was examined for two initial concentrations of AMX, 0.0136 and 0.082 mM. The corresponding results are presented in Figure 8(a) and 8(b), respectively. When the initial concentration of AMX was 0.0136 mM, the corresponding initial BOD_5/COD ratio was 0.07, which diminished to reach 0 after 60 min of reaction time, as demonstrated in Figure 8(a). A total removal of AMX was obtained within 90 min of pretreatment (Figure 5), the corresponding COD abatement and BOD_5/COD ratio were 50% and 0.36, respectively.

From the results displayed in Figure 8(b), it can be seen that the BOD_5/COD ratio of the AMX solution (before treatment) was 0.01, indicating very low biodegradability. During electro-Fenton treatment, the removal of refractory contaminants can be achieved by means of hydroxyl radicals, which break down the parent molecules of the pollutants into more biodegradable intermediates which are more easily degraded by microorganisms. As a result, the biodegradability was improved to 0.22 after 2 hours of reaction time and the corresponding COD abatement yield reached 82.3%.

To understand the low biodegradability of the degradation by-products generated during the oxidation process, the related literature was explored. Trovó *et al.* (2011) studied the degradation of AMX by the photo-Fenton process, they noticed that the intermediates generated during treatment are more toxic than the AMX. The results indicated that diketopiperazine-2,5 is the principle degradation product of AMX. The same finding was reported by Lamm *et al.* (2009). The photocatalytic degradation of amoxicillin was investigated by Çağlar Yılmaz *et al.* (2020), the identification of the degradation by-products revealed the formation of two main products: phenol followed by benzene. These two compounds are known to be toxic. This clearly explains the low biodegradability of the electrolyzed solutions of amoxicillin. The increase of the BOD_5/COD ratio after the electro-Fenton treatment indicates that a biological treatment could be envisaged, even though the limit of biodegradability, 0.4, was not attained (Carboneras Contreras *et al.* 2020). However, the COD abatement corresponding was 82.3%, which suggests that a large amount of organic matter had been oxidized. From this, subsequent biological treatment may not be relevant for the degradation of AMX by-products owing to their low biodegradability and the high oxidation of the solution, namely the low organic compounds remaining in the solution.

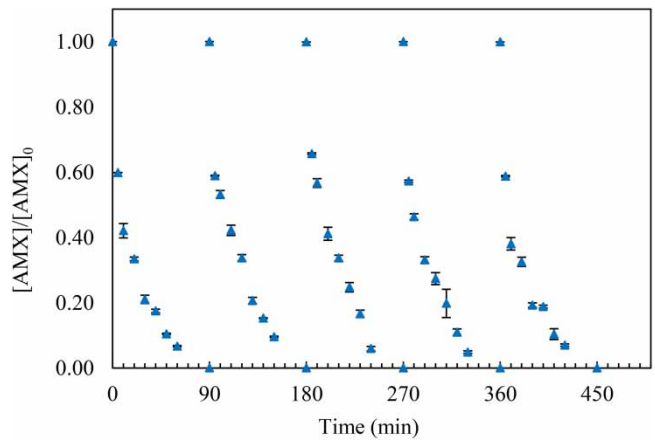

Figure 7 | Fe-Alg reusability for the degradation of AMX. Conditions: I = 600 mA, $[Na_2SO_4]$ = 50 mM, $[AMX]_0$ = 0.0136 mM, pH = 3, T = 25 °C, ω = 360 rpm.

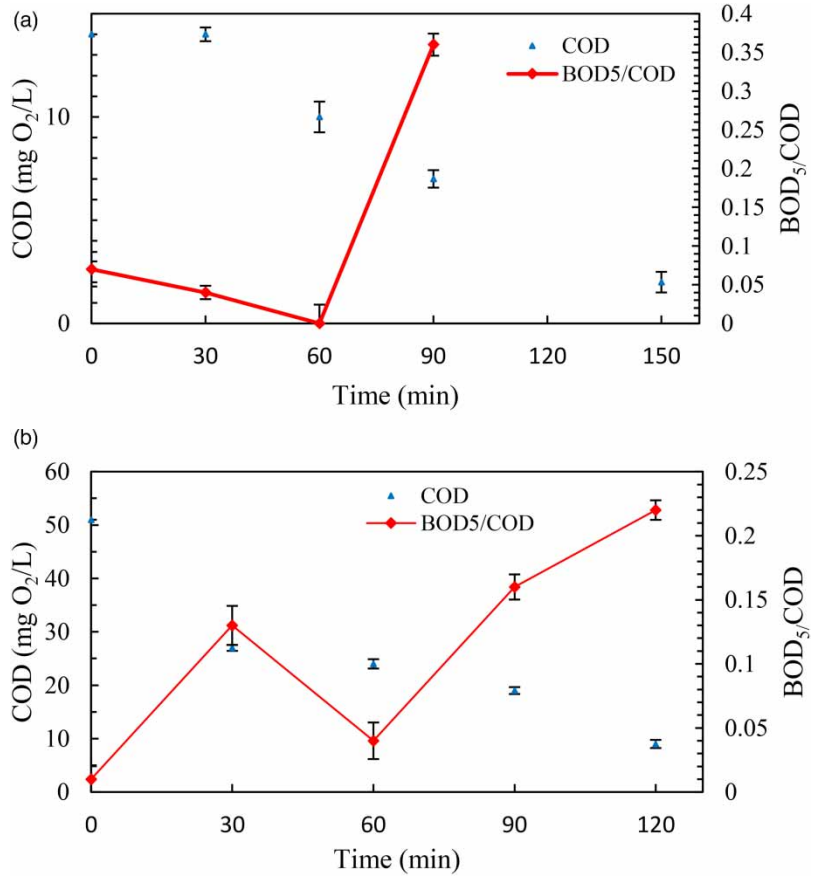

Figure 8 | Evolution of the biodegradability. Conditions : I = 600 mA, $[Na_2SO_4]$ = 50 mM, pH = 3, T = 25 °C, ω = 360 rpm. (a) $[AMX]_0$ = 0.0136 mM, (b) $[AMX]_0$ = 0.082 mM).

CONCLUSION

Developing stable, active and efficient catalyst material for environmental application is necessary. In this work, the synthesis, characterization and the application of iron supported by alginate material were reported in this study. The iron content of the Fe-Alg beads was determined to be 4.63% w/w. The use of this heterogeneous catalyst demonstrated its efficiency in overcoming excess iron ions. Indeed, after 5 cycles of use, the depletion of the Alg-Fe catalyst was only 8%, and thus the amount of sludge generated is reduced.

Furthermore, a complete degradation of AMX by the electro-Fenton treatment was obtained after 5 degradation cycles under the following conditions: initial AMX concentration 0.0136 mM, 600 mA current intensity, and 90 minutes of reaction time. In addition, a removal efficiency of 100% and a COD reduction of 85.7% were obtained after only 90 and 150 minutes of reaction time, respectively.

The results of the kinetic modelling using the non-linear method showed that at low concentration, the degradation reaction follows a pseudo-second-order kinetic. Biodegradability tests showed that after treating the AMX solution with the electro-Fenton process, the biodegradability ratio (BOD_5/COD) was increased from 0.07 to 0.36 namely close to the limit threshold (0.4) revealed the improvement of the biodegradability of the solution.

The results obtained in the present study indicate that the heterogeneous electro-Fenton process is an efficient method for the removal of refractory organic compounds.

DATA AVAILABILITY STATEMENT

All relevant data are included in the paper or its Supplementary Information.

REFERENCES

Aissani, T., Yahiaoui, I., Boudrahem, F., Ait Chikh, S., Aissani-Benissad, F. & Amrane, A. 2018 The combination of photocatalysis process (UV/TiO_2 (P25) and UV/ZnO) with activated sludge culture for the degradation of sulfamethazine. *Separation Science and Technology* **53** (9), 1423–1433. https://doi.org/10.1080/01496395.2018.1445109.

Akkouche, F., Boudrahem, F., Yahiaoui, I., Vial, C., Audonnet, F. & Aissani-Benissad, F. 2021 Cotton textile waste valorisation for removal of tetracycline and paracetamol alone and in mixtures from aqueous solutions: effects of H_3PO_4 as an oxidizing agent. *Water Environment Research* **93**, 464–478. doi:10.1002/wer.1449.

Ammar, S., Oturan, M. A., Labiadh, L., Guersalli, A., Abdelhedi, R., Oturan, N. & Brillas, E. 2015 Degradation of tyrosol by a novel electro-Fenton process using pyrite as heterogeneous source of iron catalyst. *Water Research* **74**, 77–87. https://doi.org/10.1016/j.watres.2015.02.006.

Annabi, C., Fourcade, F., Soutrel, I., Geneste, F., Floner, D., Bellakhal, N. & Amrane, A. 2016 Degradation of enoxacin antibiotic by the electro-Fenton process: optimization, biodegradability improvement and degradation mechanism. *Journal of Environmental Management* **165**, 96–105. https://doi.org/10.1016/j.jenvman.2015.09.018.

Antonin, V. S., Santos, M. C., Garcia-Segura, S. & Brillas, E. 2015 Electrochemical incineration of the antibiotic ciprofloxacin in sulfate medium and synthetic urine matrix. *Water Research* **83**, 31–41. https://doi.org/10.1016/j.watres.2015.05.066.

Aramyan, S. M. & Moussavi, M. 2017 Advances in fenton and fenton based oxidation processes for industrial effluent contaminants control-a review. *International Journal of Environmental Sciences & Natural Resources* **2** (4). https://doi.org/10.19080/ijesnr.2017.02.555594.

Boudrahem, F., Yahiaoui, I., Saidi, S., Yahiaoui, K., Kaabache, L., Zennache, M. & Aissani-Benissad, F. 2019 Adsorption of pharmaceutical residues on adsorbents prepared from olive stones using mixture design of experiments model. *Water Science and Technology* **80**, 998–1009. https://doi.org/10.2166/wst.2019.346.

Çağlar Yılmaz, H., Akgeyik, E., Bougarrani, S., El Azzouzi, M. & Erdemoğlu, S. 2020 Photocatalytic degradation of amoxicillin using Co-doped TiO_2 synthesized by reflux method and monitoring of degradation products by LC–MS/MS. *Journal of Dispersion Science and Technology* **41** (3), 414–425. https://doi.org/10.1080/01932691.2019.1583576.

Carboneras Contreras, M. B., Villaseñor Camacho, J., Fernández-Morales, F. J., Cañizares, P. C. & Rodrigo Rodrigo, M. A. 2020 Biodegradability improvement and toxicity reduction of soil washing effluents polluted with atrazine by means of electrochemical pre-treatment: influence of the anode material. *Journal of Environmental Management* **255**, 109895. https://doi.org/10.1016/j.jenvman.2019.109895.

Dogan, S. & Kidak, R. 2016 A plug flow reactor model for UV-based oxidation of amoxicillin. *Desalination and Water Treatment* **57** (29), 13586–13599. https://doi.org/10.1080/19443994.2015.1058728.

Elizalde-Velázquez, A., Gómez-Oliván, L. M., Galar-Martínez, M., Islas-Flores, H., Dublán-García, O. & SanJuan-Reyes, N. 2016 Amoxicillin in the aquatic environment, its fate and environmental risk. In: *Environmental Health Risk – Hazardous Factors to Living Species* (Larramendy, M. & Soloneski, S., eds). InTech. https://doi.org/10.5772/62049.

Fundueanu, G., Nastruzzi, C., Carpov, A., Desbrieres, J. & Rinaudo, M. 1999 Physico-chemical characterization of Ca-alginate microparticles produced with different methods. *Biomaterials* **20** (15), 1427–1435. http:/doi: 10.1016/s0142-9612(99)00050-2.

Ghanbari, F. & Moradi, M. 2015 A comparative study of electrocoagulation, electrochemical Fenton, electro-Fenton and peroxi-coagulation for decolorization of real textile wastewater: electrical energy consumption and biodegradability improvement. *Journal of Environmental Chemical Engineering* **3** (1), 499–506. https://doi.org/10.1016/j.jece.2014.12.018.

Hammouda, S. B., Fourcade, F., Assadi, A., Soutrel, I., Adhoum, N., Amrane, A. & Monser, L. 2016 Effective heterogeneous electro-Fenton process for the degradation of a malodorous compound, indole, using iron loaded alginate beads as a reusable catalyst. *Applied Catalysis B: Environmental* **182**, 47–58. https://doi.org/10.1016/j.apcatb.2015.09.007.

Huang, D., Hu, C., Zeng, G., Cheng, M., Xu, P., Gong, X., Wang, R. & Xue, W. 2017 Combination of Fenton processes and biotreatment for wastewater treatment and soil remediation. *Science of the Total Environment* **574**, 1599–1610. https://doi.org/10.1016/j.scitotenv.2016.08.199.

Ifelebuegu, A. O., Ukpebor, J. & Nzeribe-Nwedo, B. 2016 Mechanistic evaluation and reaction pathway of UV photo-assisted Fenton-like degradation of progesterone in water and wastewater. *International Journal of Environmental Science and Technology* **13** (12), 2757–2766. https://doi.org/10.1007/s13762-016-1103-3.

Iglesias, O., Gómez, J., Pazos, M. & Sanromán, M. Á. 2014 Electro-Fenton oxidation of imidacloprid by Fe alginate gel beads. *Applied Catalysis B: Environmental* **144**, 416–424. https://doi.org/10.1016/j.apcatb.2013.07.046.

Ikhlef-Taguelmimt, T., Hamiche, A., Yahiaoui, I., Bendellali, T., Lebik-Elhadi, H., Ait-Amar, H. & Aissani-Benissad, F. 2020 Tetracycline hydrochloride degradation by heterogeneous photocatalysis using TiO_2 (P25) immobilized in biopolymer (Chitosan) under UV irradiation. *Water Science and Technology* **82**, 1570–1578. https://doi.org/10.2166/wst.2020.432.

Kadji, H., Yahiaoui, I., Garti, Z., Amrane, A. & Aissani-Benissad, F. 2021 Kinetic degradation of amoxicillin by using the electro-Fenton process in the presence of a graphite rods from used batteries. *Chinese Journal of Chemical Engineering* **32**, 183–190. https://doi.org/10.1016/j.cjche.2020.08.032.

Kalantary, R. R., Farzadkia, M., Kermani, M. & Rahmatinia, M. 2018 Heterogeneous electro-Fenton process by Nano-Fe3O4 for catalytic degradation of amoxicillin: process optimization using response surface methodology. *Journal of Environmental Chemical Engineering* **6** (4), 4644–4652. https://doi.org/10.1016/j.jece.2018.06.043.

Kumar, V., Prasad, R. & Kumar, M. 2021 Rhizobiont in bioremediation of hazardous waste. In: *Rhizobiont in Bioremediation of Hazardous Waste. Chapter 21*. https://doi.org/10.1007/978-981-16-0602-1.

Lamm, A., Gozlan, I., Rotstein, A. & Avisar, D. 2009 Detection of amoxicillin-diketopiperazine-2′, 5′ in wastewater samples. *Journal of Environmental Science and Health, Part A* **44** (14), 1512–1517. https://doi.org/10.1080/10934520903263306.

Li, M., Zeng, Z., Li, Y., Arowo, M., Chen, J., Meng, H. & Shao, L. 2015 Treatment of amoxicillin by O 3 /Fenton process in a rotating packed bed. *Journal of Environmental Management* **150**, 404–411. https://doi.org/10.1016/j.jenvman.2014.12.019.

Liu, D., Zhang, H., Wei, Y., Liu, B., Lin, Y., Li, G. & Zhang, F. 2018 Enhanced degradation of ibuprofen by heterogeneous electro-Fenton at circumneutral pH. *Chemosphere* **209**, 998–1006. https://doi.org/10.1016/j.chemosphere.2018.06.164.

Madi-Azegagh, K., Yahiaoui, I., Boudrahem, F., Aissani-Benissad, F., Vial, C., Audonnet, F. & Favier, L. 2018a Applied of central composite design for the optimization of removal yield of the ketoprofen (KTP) using electrocoagulation process. *Separation Science and Technology*, 3115–3127. https://doi.org/10.1080/01496395.2018.1556298.

Madi-Azegagh, K., Aissani-Benissad, F. & Yahiaoui, I. 2018b Treatment of medical waste using electrocoagulation process. In: *Proceedings of the Third International Symposium on Materials and Sustainable Development* (Abdelbaki, B., Safi, B. & Saidi, M., eds) Springer International Publishing, Cham, pp. 527–539. https://doi.org/10.1007/978-3-319-89707-3_57.

Mansour, D., Fourcade, F., Bellakhal, N., Dachraoui, M., Hauchard, D. & Amrane, A. 2012 Biodegradability improvement of sulfamethazine solutions by means of an electro-Fenton process. *Water, Air, & Soil Pollution* **223** (5), 2023–2034. https://doi.org/10.1007/s11270-011-1002-7.

Miklos, D. B., Remy, C., Jekel, M., Linden, K. G., Drewes, J. E. & Hübner, U. 2018 Evaluation of advanced oxidation processes for water and wastewater treatment – a critical review. *Water Research* **139**, 118–131. https://doi.org/10.1016/j.watres.2018.03.042.

Mirzaei, A., Chen, Z., Haghighat, F. & Yerushalmi, L. 2017 Removal of pharmaceuticals from water by homo/heterogonous Fenton-type processes – a review. *Chemosphere* **174**, 665–688. https://doi.org/10.1016/j.chemosphere.2017.02.019.

Mojiri, A., Vakili, M., Farraji, H. & Aziz, S. Q. 2019 Combined ozone oxidation process and adsorption methods for the removal of acetaminophen and amoxicillin from aqueous solution; kinetic and optimisation. *Environmental Technology & Innovation* **15**, 100404. https://doi.org/10.1016/j.eti.2019.100404.

Nayebi, B. & Ayati, B. 2021 Degradation of emerging amoxicillin compound from water using the electro-fenton process with an aluminum anode. *Water Conservation Science and Engineering* **6** (1), 45–54. https://doi.org/10.1007/s41101-021-00101-4.

Rezgui, S., Amrane, A., Fourcade, F., Assadi, A., Monser, L. & Adhoum, N. 2018 Electro-Fenton catalyzed with magnetic chitosan beads for the removal of Chlordimeform insecticide. *Applied Catalysis B: Environmental* **226**, 346–359. https://doi.org/10.1016/j.apcatb.2017.12.061.

Rosales, E., Iglesias, O., Pazos, M. & Sanromán, M. A. 2012 Decolourisation of dyes under electro-Fenton process using Fe alginate gel beads. *Journal of Hazardous Materials* **213–214**, 369–377. https://doi.org/10.1016/j.jhazmat.2012.02.005.

Saidi, S., Boudrahem, F., Yahiaoui, I. & Aissani-Benissad, F. 2019 Agar-agar impregnated on porous activated carbon as a new adsorbent for Pb(II) removal. *Water Science and Technology* **79** (7), 1316–1326. https://doi.org/10.2166/wst.2019.128.

Saywell, L. G. & Cunningham, B. B. 1937 Determination of iron: colorimetric o-phenanthroline method. *Industrial & Engineering Chemistry Analytical Edition* **9** (2), 67–69. https://doi.org/10.1021/ac50106a005.

Taoufik, N., Boumya, W., Achak, M., Sillanpää, M. & Barka, N. 2021 Comparative overview of advanced oxidation processes and biological approaches for the removal pharmaceuticals. *Journal of Environmental Management* **288**. https://doi.org/10.1016/j.jenvman.2021.112404

Trovó, A. G., Pupo Nogueira, R. F., Agüera, A., Fernandez-Alba, A. R. & Malato, S. 2011 Degradation of the antibiotic amoxicillin by photo-Fenton process – chemical and toxicological assessment. *Water Research* **45** (3), 1394–1402. https://doi.org/10.1016/j.watres.2010.10.029.

Yahiaoui, I., Aissani-Benissad, F., Fourcade, F. & Amrane, A. 2016 Enhancement of the biodegradability of a mixture of dyes (methylene blue and basic yellow 28) using the electrochemical process on a glassy carbon electrode. *Desalination and Water Treatment* **57** (26), 12316–12323. https://doi.org/10.1080/19443994.2015.1046944.

Yahiaoui, I., Yahia Cherif, L., Madi, K., Aissani-Benissad, F., Fourcade, F. & Amrane, A. 2018 The feasibility of combining an electrochemical treatment on a carbon felt electrode and a biological treatment for the degradation of tetracycline and tylosin – application of the experimental design methodology. *Separation Science and Technology* **53** (2), 337–348. https://doi.org/10.1080/01496395.2017.1385626.

Zárate-Guzmán, A. I., González-Gutiérrez, L. V., Godínez, L. A., Medel-Reyes, A., Carrasco-Marín, F. & Romero-Cano, L. A. 2019 Towards understanding of heterogeneous Fenton reaction using carbon-Fe catalysts coupled to in-situ H2O2 electro-generation as clean technology for wastewater treatment. *Chemosphere* **224**, 698–706. https://doi.org/10.1016/j.chemosphere.2019.02.101.

Zhao, J., Sun, Y., Wu, F., Shi, M., Liu, X. & Meca, G. 2019 Oxidative degradation of amoxicillin in aqueous solution by thermally activated persulfate. *Journal of Chemistry*. https://doi.org/10.1155/2019/2505823.

First received 24 November 2021; accepted in revised form 21 February 2022. Available online 7 March 2022